International Refrigeration and Air Conditioning Conference | School of Mechanical Engineering

2022

Advanced Copper Heat Exchangers from Low-Cost Additive Manufacturing Techniques

Dennis Michael Nasuta

Austin Halota

Angelina Zhao

Max Mzhen

Advanced Copper Heat Exchangers from Low-Cost Additive Manufacturing Techniques

Dennis NASUTA*, Austin HALOTA, Angelina ZHAO, Max MZHEN

Optimized Thermal Systems, Inc.
Beltsville, MD, USA
nasuta@optimizedthermalsystems.com

* Corresponding Author

ABSTRACT

Heat exchanger designs continue to evolve in response to pressures to reduce thermal and hydraulic resistances, environmental impacts, and costs. Inevitably, these forces yield increasingly miniaturized designs having high surface area to volume ratios and often novel geometries. More compact and exotic heat exchangers have been demonstrated to outperform the current state of the art, but techniques to fabricate these advanced designs remain limited. Current high production volume techniques are too constrained to produce next generation designs; conversely, metal additive manufacturing can produce highly complex geometries, but is often too costly and time-consuming. Taking inspiration from the manufacture of metallic microlattices, a low-cost technique was developed to create functional metallic heat exchangers with conventional materials and consumer-grade products. The fabrication process begins with 3D printing a polymer part on an FDM/FFF or SLA machine. The part is then prepared and electroplated with copper until a sufficiently thick layer of metal has accumulated. Polymer can then be removed from the interior of the part by melting or with a solvent. This process has been used successfully to fabricate sample heat exchangers with flow channel diameters less than 1mm and complex geometries unobtainable through conventional (tube fin or microchannel) manufacturing processes. At present, the technique provides an exciting capability allowing engineers to rapidly fabricate and test novel heat exchanger geometries as prototype or low-volume parts. Future innovations may improve the processes for additive manufacturing, plating, and cleaning parts, further expanding the scale of applications for which the technique can be applied.

1. INTRODUCTION

Heat exchangers remain critical components driving the energy efficiency of a wide range of thermal systems in HVAC&R and beyond. Today, essentially all products operate well below their theoretical maximum Carnot COPs in large part due to their need to exchange heat across large temperature gradients resulting from thermal resistances in heat exchangers. Given unlimited space and material resources, these irreversibilites due to heat exchange can be minimized, but actual products constrained by cost and consumer acceptance compromise on performance with non-ideal heat exchangers (HXs). In the past few decades, researchers have continued to pursue heat exchanger designs that can increase thermal conductance while minimizing material and/or size, yet nearly all HVAC&R products continue to use the same tube-fin or microchannel heat exchanger technology due to the high cost and complexity of developing new manufacturing capabilities.

The evolution of heat exchanger design has shown a clear trend towards smaller feature sizes and flow channels. This is often attributed to simple geometry scaling: as tube diameters decrease, the ratio of outer heat transfer surface area to material consumption or overall volume increases as shown in Figure 1 by Bacellar (2016). Industry has adopted designs with increasingly small diameter flow channels, as some manufacturers have implemented microchannels and 5mm OD tube fin heat exchangers in replacement of conventional 3/8" or larger diameter tubes. These boundaries are pushed further towards this limit with so-called "microtube" heat exchangers having diameters less than 1mm. These microtube designs may be the most compact among current state of the art HX manufacturing processes.
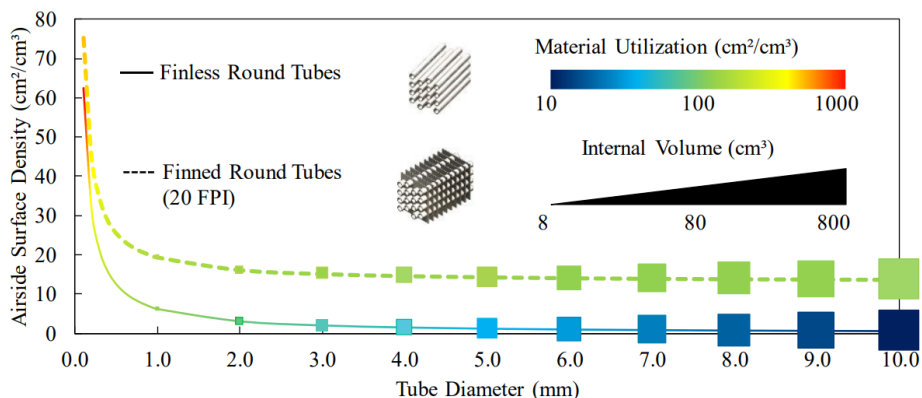
Figure 1:First-order assessment of HX flow channel diameters (Bacellar, 2016)

In order to further improve performance, it is useful to evaluate designs and manufacturing techniques beyond the conventional assembly of extruded tubes with or without fins. Numerous research papers have been published exploring novel HX geometries that dramatically improve performance but require new manufacturing techniques. Many authors have looked to direct metal additive manufacturing as a technique to produce novel heat exchangers with 3-dimensional complexity that would be unachievable through other means. Bacellar et al. (2017) designed a shape-optimized heat exchanger with droplet-shaped tubes with about 40% higher HTC and 18% lower ΔP and printed it in titanium and tested it experimentally (Figure 2A). Even more exotic geometries (Figure 2) have been devised through topology optimization where 3D printing unlocks a new dimension of design possibilities that could be produced by no other means (Figure 2B, Vlahinos & O'Hara, 2020). Other interesting 3D HX geometries can be seen in Son et al. (2017) and Dixit et al. (2022), among others.
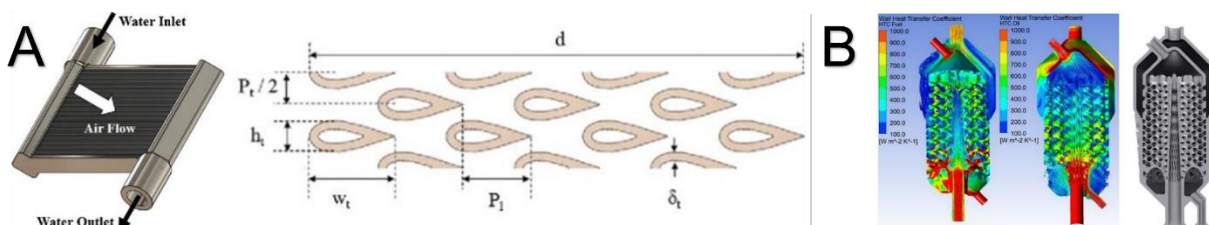
Figure 2: (A) NURBS tube shape optimized heat exchanger (Bacellar et al., 2017) and (B) Aviation fuel cooled oil cooler with TPMS geometry (Vlahinos & O'Hara, 2020).

Such complex 3D printed products are beginning to enter the market in real applications, but their adoption is very limited; the high cost and low throughput of these techniques have meant that aviation and spacecraft applications primarily utilize these components in final products. While ongoing progress continues to drive down the costs of additive manufacturing, it is far from achieving the costs and speeds required for high production volume components like HVAC&R heat exchangers. However, 3D printing does have the capability to drastically improve the R&D process of new heat transfer surfaces. Furthermore, there may be opportunities to develop new, lower-cost "hybrid" techniques that make use of additive manufacturing in combination with more established conventional manufacturing approaches.

2. INSPIRATION AND APPROACH

The present work grows from a desire to explore these next generation heat exchanger designs using more accessible fabrication techniques. More than a decade ago, researchers developed a technique to produce so-called "ultralight metallic microlattices" and numerous subsequent articles proclaimed the remarkable strength to weight ratio of these parts (Schaedler et al., 2011). The procedure for producing microlattices (Figure 3) consists of the fabrication of a photopolymer part cured with UV light which is then plated with a layer of metal. Importantly, rather than using a layer-by-layer stereolithography technique, these polymer parts are made using self-propagating waveguides, which allow for faster and more scalable production. The polymer is then dissolved out of the part leaving a hollow metal structure that is extremely lightweight and surprisingly strong. While this technique has been considered for various

aerospace and vehicular applications, it is also attractive for heat exchangers because of the ability to produce small flow channels with potentially smaller feature sizes, lower cost, and less specialized equipment than current metal additive manufacturing techniques.
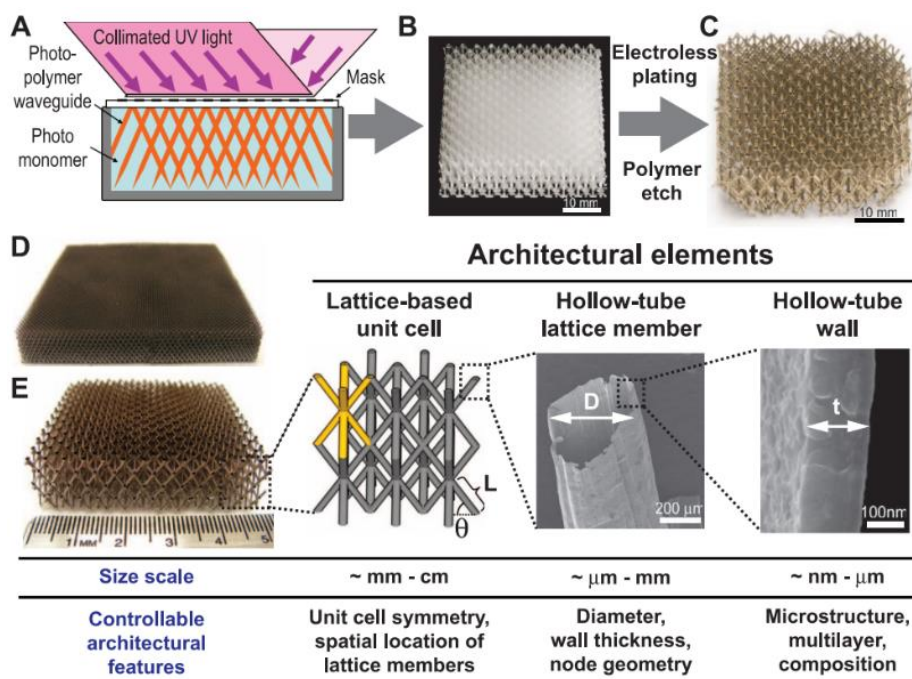
Figure 3: Ultralight metallic microlattices (Schaedler et al., 2011)

3D printing in polymers has become eminently accessible with consumer fused deposition modeling (FDM)/fused filament fabrication (FFF) and stereolithography (SLA) machines costing only hundreds of dollars. The process of metal plating polymer parts, either through electro- or electroless-plating, is well-established to the extent that it is common among 3D printing hobbyists using consumer equipment. In fact, the process of producing microlattices has already been replicated using consumer equipment (Breaking Taps, 2020). The intent of this work is to establish that these techniques can also be used to create functional heat exchangers using only consumer equipment that cannot be manufactured by conventional means.

3. MATERIALS AND METHODS

The fabrication of plated copper heat exchangers was accomplished through the following steps. Multiple alternative techniques exist at each stage of the procedure and the discussion of possibilities is not comprehensive.
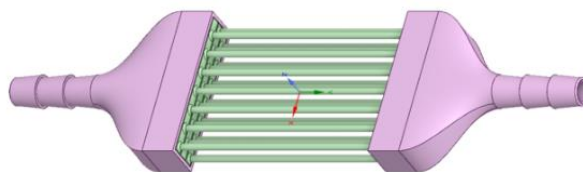
Figure 4: Complete heat exchanger assembly in CAD including plating and fit tolerances featuring three tube banks (green) and both inlet and outlet manifolds (purple).

1. Design heat exchanger part in CAD. The process begins with the creation of the heat exchanger geometry in a CAD program. The parts to be plated are modeled as solid parts with no gaps, which represent the void volumes of the plated heat exchanger parts. The thickness added to the outer surface by the copper plating is considered in the design, as are the tolerances between adjacent parts. The functional prototype design (Figure 4) uses three banks of tubes in a staggered arrangement with plastic manifolds to join them. The tubes are to

be plated, so the ID of the part is modeled. The manifolds (purple) are modeled with their actual wall thickness and void volumes. They have hose barbs to interface with ¼" ID vinyl tubing.

2. Print polymer part. Both SLA and FDM methods can be used. In this sample, a consumer grade FDM printer was used to create a part in Polyvinyl alcohol (PVA) for ease of dissolution, though Polylactic acid (PLA) has also been used.

3. Coat polymer part with conductive paint. It is necessary to coat the printed polymer parts with an electrically conductive material before plating. The conductive coating can be made with a suspension of carbon graphite powder in paint or lacquer which is then applied with a brush or by dipping. Alternatively, commercially available conductive aerosol paint designed for EMI shielding can be sprayed on the parts (Figure 5). The step of applying conductive paint to the parts before plating might be eliminated with electroless plating techniques or by printing the parts with electrically conductive filaments (Kim et al., 2019).
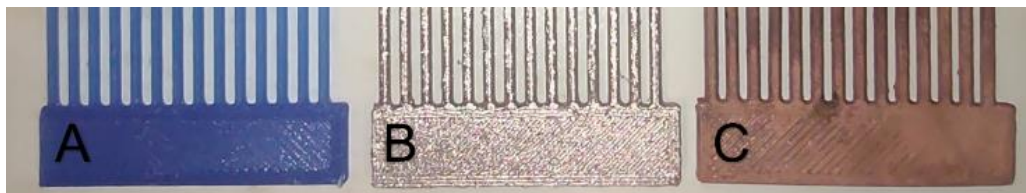
Figure 5: Part surface in different stages of process: (A) polymer part (B) polymer part coated with conductive paint (C) part after plating and removing polymer to leave only the copper shell.

4. Plate part with metal. For this effort, an electroplating solution (Table 1) was prepared with distilled water, copper sulfate pentahydrate, and sulfuric acid. A benchtop variable DC power supply was used to control the copper deposition rate while plating, and the solution was constantly agitated with a magnetic stirrer. Parts were suspended in the solution with many points of contact from bare copper wire connected to the negative lead of the DC power supply. The amount of time and current used for plating depended on the surface area of the parts among other process parameters. Lower current densities < 10 mA/cm^2 were used to improve plating thickness consistency and surface finish: these settings required ~12-16 hours of total plating time with agitation to achieve target copper thicknesses of ~0.2 mm. Current density also has a significant impact on surface quality and the process parameters employed in this proof of concept are not yet optimized.

Table 1: Electrolyte solution preparation.

Chemical	Note	Quantity	Unit
Deionized or distilled water	-	1000	mL
Copper Sulfate Pentahydrate (CuSO$_4$ • 5H$_2$O)	Crystalline powder form	200	g
Concentrated sulfuric acid (H$_2$SO$_4$)	Drain cleaner (concentrated)	40	mL

5. Remove polymer interior. Following plating, the internal polymer material must be removed to form the flow channel for the tube-side fluid. Two different concepts were explored in this effort to produce a shelled copper part. Both methods required first sanding or drilling an opening through the copper plating of the part to expose the polymer interior. The first method was to liquify and vaporize PLA out of the part in a kiln. This worked well for parts with larger features and tube diameters, but parts with smaller features and tube diameters often deformed or ruptured during the thermal removal process (Figure 6B). The design of the flow channels and headers influenced the success of the process: when PLA inside the smaller tubes vaporized before the headers, the increased pressure could burst tubes. A butane torch was later used to give more precise control to the process by removing material from the manifolds first, but the process was delicate and tedious, and the failure rate was still high. The thermal removal process could be improved by adding temperature controls to the kiln, using different polymer materials, insulating the tubes, and re-designing the parts to facilitate gas escape.

The second method was to dissolve PVA out of the copper shell with hot water and agitation. The parts would be left in 90-100°C water with constant mechanical stirring for ~30 hours with multiple water changes to completely dissolve the PVA (confirmed by visual inspection). This method was found to be more reliable for small tube diameters (< 2mm OD). Both methods described were successful in creating hollow channels in copper plated parts; however, these methods can be improved further with experimentation with different materials, solvents, and processes (e.g., ultrasonic baths).

4. INITIAL RESULTS

4.1 Proof of Concept Prototypes

The steps above were followed successfully to create functional parts that could be used to transfer heat. Early exploratory tests produced a manifold sample (Figure 6) with flow channel diameters ranging from 1 to 6mm and material thickness up to 0.4mm. After process parameters were established in this proof of concept, additional heat exchangers were fabricated.
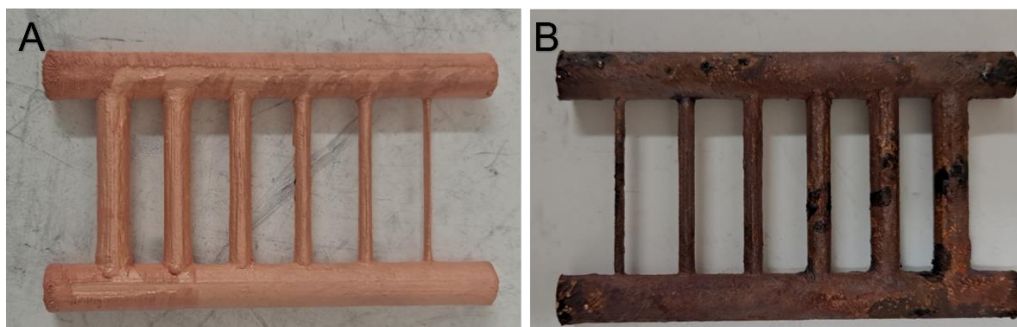
Figure 6: Early prototype with tubes and manifolds (A) immediately after plating and (B) after kiln firing. The flow channels range from 1-6mm (CAD/inner dimension) in diameter in 1mm increments.

4.2 Functional Prototypes

The prototype design was developed into a functional heat exchanger (Figure 7). It was designed to be printed, plated, and assembled rapidly while process parameters were being refined, and the following results show the best outcome obtained with the current process. The tube banks were printed out of PVA, coated with polyurethane, coated with conductive paint, plated, and the polymer interior dissolved in hot water to shell the copper part. Manifolds were printed out of PLA to join three banks into a staggered tube arrangement with a single pass parallel flow configuration, merging the tube inlets/outlets into ¼" ID hose barbs. The internal and external finish of the parts is acceptable, as shown in Figure 7. The nominal flow channel diameter of the tubes is 1.6mm, and the plating thickness varies from 0.20-0.27mm (Table 2 provides geometry details in tabular format).
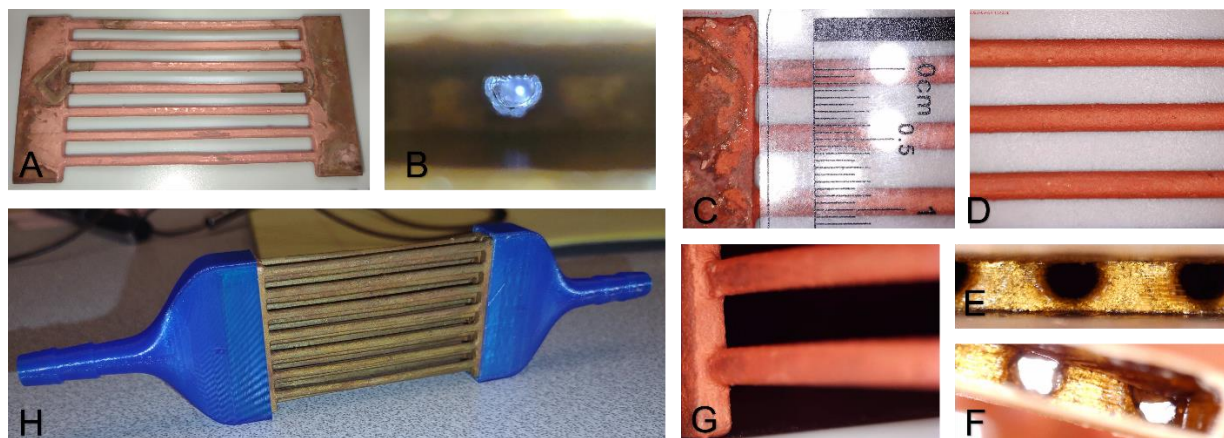
Figure 7: Images of functional prototype: (A) single tube bank after shelling (B) unobstructed flow channel with all polymer dissolved; microscope images of (C) manifold and tubes with calibration gauge (D) surface roughness on tube outer diameter (E) view into manifold without backlight with apparent layer lines from 3D printing (F) view into manifold with backlighting (G) angled view of tubes where they join the manifold; (H) assembled prototype before applying sealant between copper parts and plastic manifolds.

Table 2: Prototype geometry as polymer part, copper plated shell, and assembled part without manifolds or sealant.

Part	Unit	Printed	Plated Shell	Assembled
Tube				
D_i	mm	-	1.60	1.60
D_o	mm	1.60	2.13	2.13
L_t	mm	50.80	50.40	50.40
Th	mm	-	0.265	0.265
General Geometry				
N_r	-	7	7	7
N_b	-	1	1	3
A_o	mm^2	1983.16	2330.73	6992.20
m	g	2.27	3.78	11.35

4.3 Initial Performance Testing

Initial performance testing was done on a miniaturized, 3D-printed, open-loop wind tunnel (Figure 8). The wind tunnel was adapted for the prototype heat exchanger with a custom inlet duct test section with a cutout for the prototype to slide into and a port to accept a tube for static pressure measurement. The prototype was sealed to the walls of the test section with duct seal compound. Prior to testing, the loop was calibrated with an energy balance method: a measured quantity of heat was added to the loop and the measured temperature difference was used to calibrate flow measurements from the pitot tube.
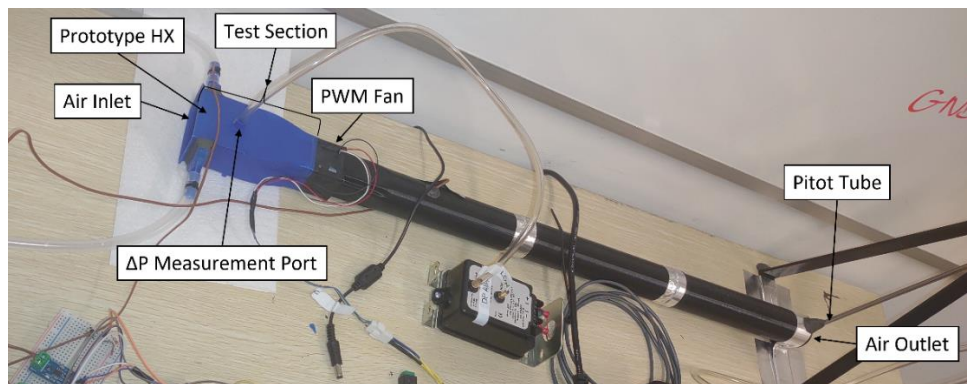
Figure 8: Wind tunnel setup with prototype heat exchanger installed.

The primary goal of the performance testing was to obtain experimental pressure drop data and compare it to predictions from CFD and a known correlation for small diameter bare tubes. The prototype was tested at a range of outlet-side air mass flows from ~6.1 to 15.6 g/s in increments of ~2 g/s. Pressure drop data (Table 3 and Figure 10) were recorded for each steady-state point for 120 seconds.

Table 3: Averaged sensor data and calculated values with statistical uncertainty at each steady-state test point.

Test #	ADP_HX [Pa]	T_air [K]	MFR* [g/s]
1	19.77 ± 0.44	296.36 ± 0.93	6.09 ± 0.17
2	61.96 ± 0.79	296.28 ± 1.00	8.37 ± 0.48
3	84.45 ± 1.09	296.27 ± 0.96	10.11 ± 0.72
4	112.65 ± 1.35	296.52 ± 0.98	12.56 ± 1.01
5	124.8 ± 1.46	296.49 ± 0.91	13.88 ± 1.35
6	141.29 ± 1.97	296.61 ± 0.91	15.61 ± 1.62

*calculated from sensor data and humid air properties

4.4 CFD Validation
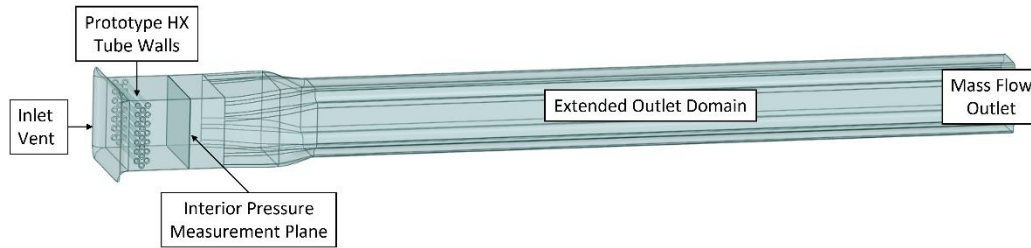
Figure 9: CFD computational domain to validate experimental velocity and pressure drop.

A parametric study was performed in CFD to compare the experimentally-observed air pressure drops against predictions. The CFD setup (Figure 9) used the outlet-side air mass flow rates measured in the experiment as the outlet (mass flow) boundary condition. The inlet boundary was configured as a vent, and all walls were treated as zero-slip boundaries. Average pressure was measured at a plane perpendicular to the fluid flow direction at the same point that the differential pressure port exists in the actual test section, and this was compared to the inlet face average pressure to calculate pressure drop across the prototype. Average velocity was calculated at the heat exchanger inlet face, which gave values between ~2.84-7.28 m/s.

Table 4: CFD results corresponding to test points 1-6.

Test #	MFR* [g/s]	ADP_HX_CFD [Pa]	ADP_HX_Experiment [Pa]	u_inlet_face_CFD [m/s]
1	6.09	23.64	19.77	2.84
2	8.37	43.94	61.96	3.91
3	10.11	63.35	84.45	4.72
4	12.56	95.60	112.65	5.86
5	13.88	115.16	124.80	6.48
6	15.61	142.81	141.29	7.28

*input as mass flow boundary condition

4.5 CoilDesigner® Validation
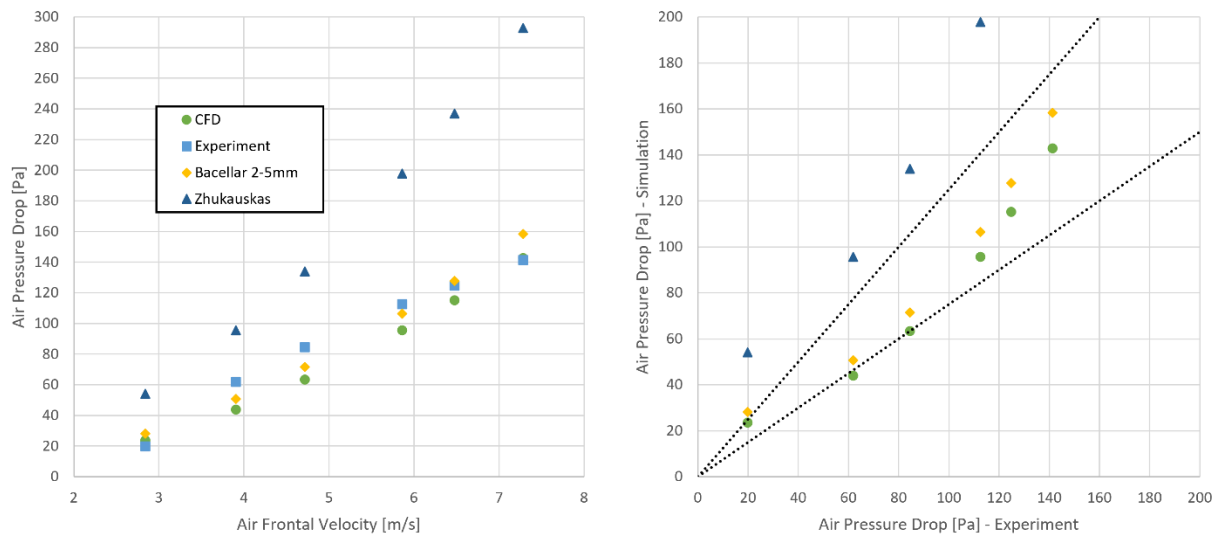
Figure 10: Airside pressure drop results (left) and air side pressure drop simulations plotted against experiment (right). Margins are ±25%.

CoilDesigner® simulations matching the test conditions were carried out using two different correlations applicable to the prototype heat exchanger geometry (Figure 10). The experimental pressure drop data are in good agreement with the CFD simulations of the prototype and the Bacellar 2-5mm correlation (2014). The CFD results and Bacellar

2-5mm correlation follow very similar trends, which is expected because the Bacellar correlation is derived from CFD data created with similar methodology. The difference in pressure drop can be partially explained by the non-uniformity of the actual geometry, the surface roughness, and the slight reduction in flow area due to the addition of sealant around the edges of the manifolds. The Žukauskas (1975) correlation overpredicts the experimentally observed pressure drop at all points.

4.6 Heat Transfer Proof of Concept

To demonstrate that the prototype heat exchanger would hold fluid and function as a heat exchanger, a quick test was configured using the wind tunnel setup shown previously (Figure 8). For the test, a thermal camera was set up to record radiometric data, and ¼" nominal inner diameter silicone tubing was connected to either end of the prototype using the integrated hose barb fittings. In the front view of the prototype, the inlet tube is connected on the left side, which is also connected to a 4W submersible aquarium pump.

With maximum air flow through the wind tunnel, hot water (~102°F) was pumped through the heat exchanger. Two areas were configured using the thermal camera software to calculate average temperatures on the exterior of the inlet and outlet manifolds, respectively, and these average temperatures were tracked for several minutes. A consistent temperature delta of up to 1.0°F was observed from the inlet manifold to the outlet manifold (Figure 11), which does indicate significant heat transfer considering the high water flow rate. Figure 12 shows the visibly warmed air passing through the walls of the wind tunnel exhaust. In future work, more precise control and measurement of flow rates may be carried out in order to determine heat transfer coefficients experimentally, but this result limited by available equipment serves to conceptually demonstrate the prototype's capability.
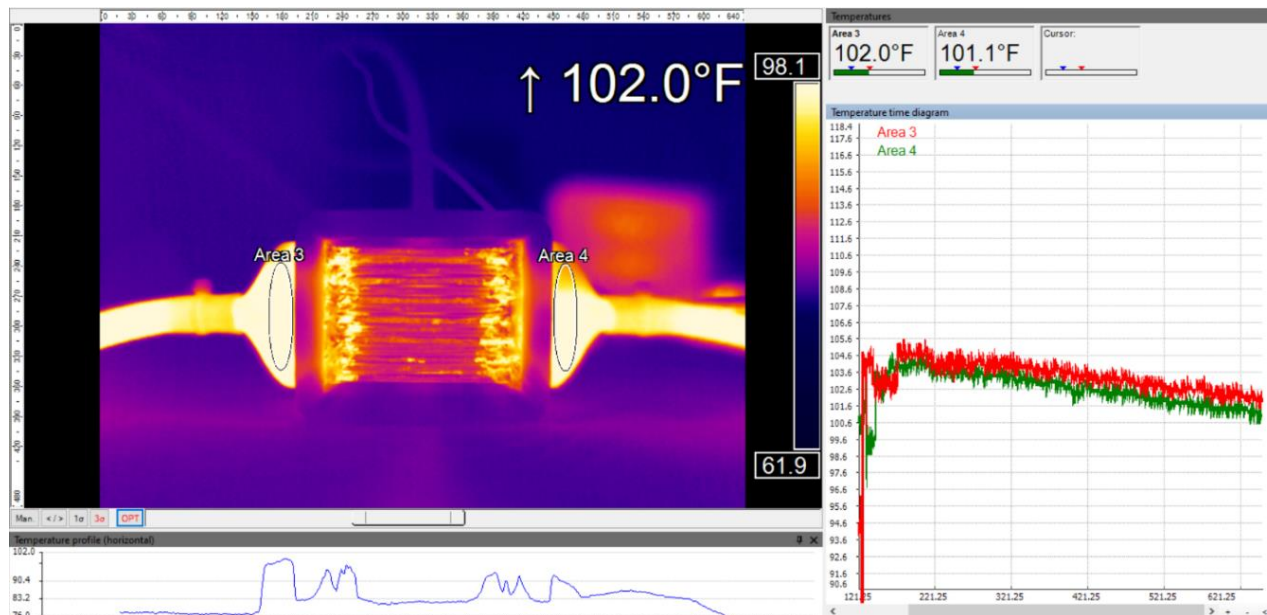
Figure 11: Thermal image of air inlet face of prototype inside test section (left). The temperature-time diagram (right) shows the rapid temperature rise after the addition of hot water to the reservoir. The temperature delta between the manifolds was maintained at ~0.9°F for several minutes.
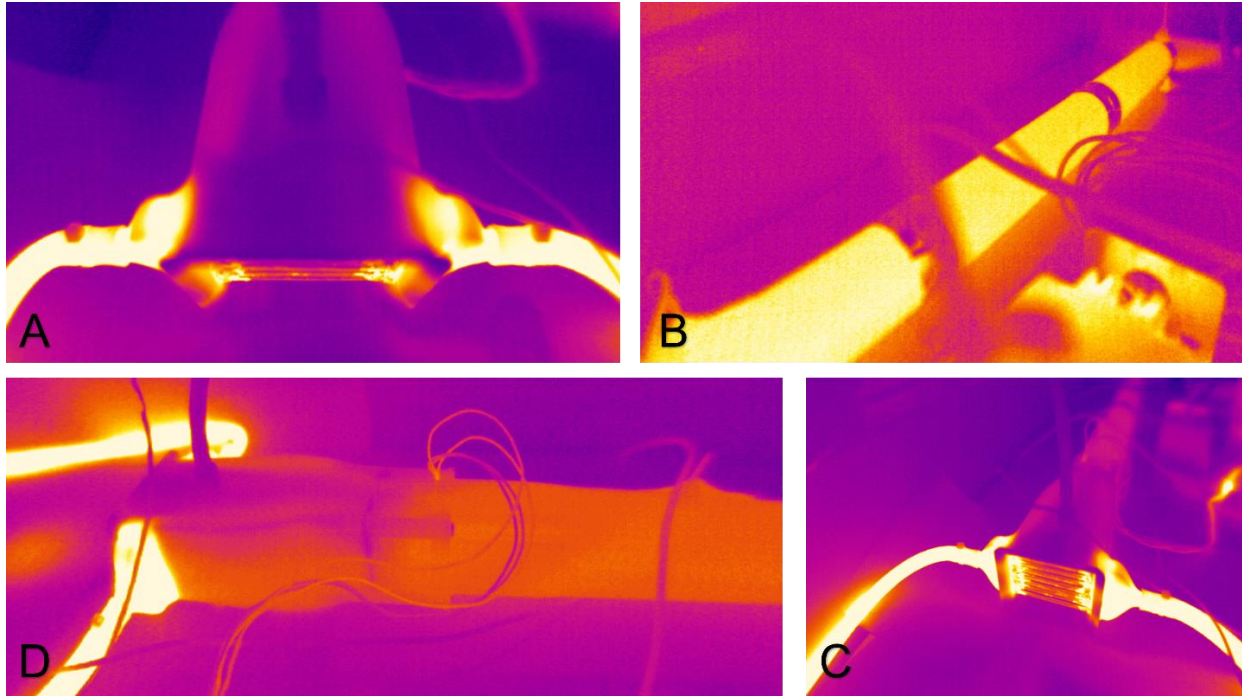
Figure 12: (A) top view looking down on intake (B) downstream exhaust tube and heating of table from exhaust air at the outlet (C) prototype in foreground with full wind tunnel in background (D) side view of test section.

5. FUTURE WORK AND POTENTIAL IMPACT

The work presented here represents only an initial exploration of a novel approach to fabricate heat exchangers that could not be produced through conventional manufacturing techniques. Additional future work should be explored to evaluate the quality of these parts and further improve the process:

- Characterization of plating quality and thickness should be performed.
- Pressure tests should be performed to determine the suitability of these parts for holding pressurized refrigerant.
- Thermal tests to determine convective heat transfer coefficients will be conducted to confirm performance of more novel geometries (e.g. non-round tubes, microlattices, fractal, or conformal HXs).
- New polymer materials should be evaluated for print quality and ease of removal.
- Conductive polymers can be explored to eliminate the need to coat parts before plating.
- Electroless plating may offer additional convenience for plating parts.
- Further optimization of plating process parameters will improve surface quality.
- Means to capture and recycle melted or dissolved polymer material will be important to ensure the sustainability of the technique.
- The use of self-propagating waveguides, as in the production of microlattices, should be explored because it may offer considerable speed and cost advantages over conventional 3D printing.

The strength of this technique lies in its ability to produce novel geometries quickly with only low-cost consumer equipment. This makes the process ideal for early prototyping and simulation validation. Researchers designing new heat exchangers through simulation-based optimization techniques can use this approach to quickly build prototypes to validate CFD simulation results at a low cost. The physical scale of parts is only limited by the bed size of the 3D printer, which can now be quite large in commercially available machines, however the feasibility of plating larger parts is limited in the typical research lab. It is not inconceivable that production-scale parts could be manufactured using this technique, but at this time, its application would be limited to low production volume parts unless a streamlined high throughput process were to be developed.

NOMENCLATURE

A	area	(mm^2)
ADP	airside pressure drop	(Pa)
D	diameter	(mm)
HTC	heat transfer coefficient	(W/m^{2}K)
ID	tube inner diameter	(mm)
L	length	(mm)
m	mass	(g)
MFR	mass flow rate	(g/s)
N	number	(-)
OD	tube outer diameter	(mm)
T	temperature	(K)
Th	thickness	(mm)
u	velocity	(m/s)

Subscript

b	banks
o	outer
r	rows
t	tube

REFERENCES

Bacellar, D. (2016). Airside Passive Heat Transfer Enhancement, using Multi-Scale Analysis and Shape Optimization, for Compact Heat Exchangers With Small Characteristic Lengths. University of Maryland, College Park.

Bacellar, D., Aute, V., Huang, Z., & Radermacher, R. (2017). Design optimization and validation of high-performance heat exchangers using approximation assisted optimization and additive manufacturing. Science and Technology for the Built Environment, 23(6), 896–911. https://doi.org/10.1080/23744731.2017.1333877

Bacellar, D., Aute, V., & Radermacher, R. (2014). CFD-Based Correlation Development For Air Side Performance Of Finned And Finless Tube Heat Exchangers With Small Diameter Tubes. International Refrigeration and Air Conditioning Conference, Purdue University. http://docs.lib.purdue.edu/cgi/viewcontent.cgi?article=2409&context=iracc

Breaking Taps. (2020, August 12). 3D printed Ultralight Metallic Microlattices. https://www.youtube.com/watch?v=tpO5DgiCgyM

Dixit, T., Al-Hajri, E., Paul, M. C., Nithiarasu, P., & Kumar, S. (2022). High performance, microarchitected, compact heat exchanger enabled by 3D printing. Applied Thermal Engineering, 210, 118339. https://doi.org/10.1016/j.applthermaleng.2022.118339

Kim, M. J., Cruz, M. A., Ye, S., Gray, A. L., Smith, G. L., Lazarus, N., Walker, C. J., Sigmarsson, H. H., & Wiley, B. J. (2019). One-step electrodeposition of copper on conductive 3D printed objects. Additive Manufacturing, 27, 318–326. https://doi.org/10.1016/j.addma.2019.03.016

Schaedler, T. A., Jacobsen, A. J., Torrents, A., Sorensen, A. E., Lian, J., Greer, J. R., Valdevit, L., & Carter, W. B. (2011). Ultralight Metallic Microlattices. Science, 334(6058), 962–965. https://doi.org/10.1126/science.1211649

Son, K. N., Weibel, J. A., Kumaresan, V., & Garimella, S. V. (2017). Design of multifunctional lattice-frame materials for compact heat exchangers. International Journal of Heat and Mass Transfer, 115, 619–629. https://doi.org/10.1016/j.ijheatmasstransfer.2017.07.073

Vlahinos, M., & O'Hara, R. (2020). Unlocking Advanced Heat Exchanger Design and Simulation with nTop Platform and ANSYS CFX. NTopology Inc., 8.

Žukauskas, A. (1975). Heat Transfer from Tubes in Cross Flow. Advances in Heat Transfer, 11.

ACKNOWLEDGEMENT